



Formulation and Evaluation of Olmesartan Medoxomil as Solid Lipid Nanoparticles and Nano Structural Lipid Carriers

Nashwa Hassan^{1*}, Shereen El-Adawy², Amal Ammar³ and Ahmed M. Samy⁴

¹Department of Pharmaceutics, Faculty of Pharmacy and Pharmaceutical Industries, Sinai University, Alarish, Egypt.

²Department of Pharmaceutics, Faculty of Pharmacy, Al Azhar University, Cairo, Egypt.

Received: 16 Jan 2019 / Accepted: 18 Mar 2019 / Published online: 1 Apr 2019

Corresponding Author Email: nashwahassan23@yahoo.com

Abstract

Objective: The aim of this work was to develop solid lipid nanoparticles (SLN) and Nanostructured lipid carrier (NLC) of an antihypertensive drug Olmesartan medoxomil (OLM) for improving its gastrointestinal uptake and oral bioavailability. **Method:** High shear homogenization coupled with ultrasonication method was used for the preparation of SLNs and NLCs formulae. Eight formulae of each system were formulated using full factorial design 2³. Three independent variables were selected. For NLCs, the variables are: type of liquid lipid (oleic acid or capryol 90) and type and concentration of surfactant (poloxamer 188 or tween 80). For SLNs, due to absence of liquid lipid, this variable was replaced by two concentrations of OLM. Morphology, particle size, and zeta potential are evaluated. Entrapment efficiency and in vitro release studies were performed using dialysis bag method. **Results:** The results showed neither incompatibility nor physicochemical reaction between the drug and the solid excipients. The particle size ranged from 219.9 to 363.5 nm and from 176.8 to 382.2 nm for SLNs and NLCs respectively. Zeta potential of all formulae were negative indicating good stability. The entrapment efficiency was found in the range of 63.23 % to 84.55 % and 77.05 to 90.64 for SLNs and NLCs respectively. The in vitro OLM release demonstrated that drug-loaded formulations gave higher drug release in controlled manner than OLM itself. **Conclusion:** The results indicated a promising potential of control release and high bioavailability of Nano particulate system. NLC are better carrier system as compared to SLN.

Keywords

Solid lipid nanoparticles, Nanostructured lipid carrier, poloxamer 188 and Olmesartan medoxomil.

INTRODUCTION

Olmesartan medoxomil is a selective AT₁ subtype angiotensin-II receptor antagonist. It acts by lowering blood pressure through arterial vasodilatation and reduced sodium retention [1]. Clinically, it is used in the treatment of hypertension. It is practically insoluble in water (<7.75 µg/ml) and rapidly absorbed from the gastrointestinal tract with peak plasma concentration of olmesartan (metabolite) occurring 1–3 h after administration. The absolute bioavailability of olmesartan from olmesartan medoxomil tablets is 28.6% with an elimination half-life of 10–15 hr [2]. Lipid nanoparticles (LNs) have been developed for various routes of administration with several objectives including enhancement of bioavailability of poor water soluble drugs.

Solid lipid nanoparticles (SLNs) and nanostructured lipid carriers (NLCs) are nanosize lipidic carriers in size range between 50 - 1000 nm, prepared with lipids and surfactants generally recognized as safe. Lipids being biodegradable, SLNs/ NLCs have excellent biocompatibility. They have combined advantages of liposome, polymeric nanoparticles and micro emulsions and avoid the drawback of several colloidal carrier of its class. Some advantages offered by SLN are good physical stability, high drug payload, controlled drug release, specific targeting, scalability and feasibility of delivering both lipophilic and hydrophilic drugs. These colloidal carriers have shown to improve bioavailability of poorly soluble drugs. SLNs by virtue of their lipophilic nature and low particle size are widely explored as a delivery system to enhance uptake throughout gastrointestinal tract [3].

NLCs are produced using blends of solid lipids and liquid lipids (oils). To obtain the blends for the particles matrix, solid lipids are mixed with liquid lipids, preferably in a ratio of 70/30 up to a ratio of 99.9/0.1. Because of the oil presence in these mixtures, a melting point depression compared to the pure solid lipid is observed, but the blends obtained are also solid at room and body temperatures [4]. They also have a significantly higher loading capacity for active ingredients [5]. Thus, there is a clinical need for a dosage form that will deliver OLM in a controlled manner to a patient needing this therapy, thereby resulting in a better patient compliance. The conventional dosage forms exhibit low bioavailability due to extensive first pass metabolism and non-targeted delivery results in numerous side effects.

The aim of this thesis was to formulate OLM in SLNs and NLCs and then study their Physico-chemical

properties and their in-vitro release, their stability and their in-vivo pattern.

In the present study, we have formulated OLM SLNs /NLCs by using Glyceryl monostearate as solid lipid base, Oleic acid or Capryol 90 as liquid lipids (oil) and Tween 80 or poloxamer 188 (0.25–5 %) as surfactants by high shear homogenization coupled with ultrasound method as an attempt for improving its gastrointestinal uptake and oral bioavailability and also to control its release.

MATERIALS AND METHODS

Materials

Olmesartan (OLM) was kindly gifted by Jedco International Pharmaceuticals (Cairo, Egypt). Glyceryl monostearate, Tween 80, Poloxamer 188 and Oleic acid was obtained from Sigma Aldrich, Mumbai, Capryol 90 was obtained Gattefosse, Germany. All other chemicals used were of analytical grade.

Methods

Preformulation Study of Olmesartan Medoxomil (OLM)

Fourier Transform Infrared spectroscopy of OLM

The compatibility study between the drug, solid lipid and emulsifier was ascertained using FTIR spectroscopy. In infrared spectroscopy, IR radiation is passed through a sample. Some of the infrared radiation is absorbed by the sample and some of it is passed through (transmitted). The resulting spectrum represents the molecular absorption and transmission, creating a molecular fingerprint of the sample. Like a fingerprint no two unique molecular structures produce the same infrared spectrum. In this analysis, six samples were analyzed; three samples composed of pure substances which are pure OLM powder, pure Glyceryl Mono Stearate (GMS) and pure Poloxamer 188 powders separately. The other three samples are mixtures: a binary physical mixture of OLM and GMS (1:1 by weight), binary mixture of OLM and Poloxamer 188 (1:1 by weight) and a ternary physical mixture of OLM, GMS and Poloxamer 188 (in ratio 1:1:1 by weight). All samples were previously ground and mixed thoroughly with spectral grade potassium bromide. The KBr discs were prepared by compressing the powders. The scanning range was from 4000–400 cm⁻¹. [6] FTIR spectra were obtained using a Shimadzu 435 U-O4 IR spectrometer.

Preliminary Differential Scanning Calorimetry analysis of OLM

Differential Scanning Calorimetry (DSC) was used to study the physical state, crystallinity and polymorphism of OLM and possible physical

interaction of it with the solid excipients to be used in the formulation. The measurement was performed by differential scanning calorimeter, Shimadzu DSC-50, (Japan). Samples weighing 2-5 mg were heated and scanned between 25° C and 250° C and a heating rate of 10° C.min⁻¹ under nitrogen gas flow (30 ml.min⁻¹) [7]. Preliminary DSC analyses were performed on the pure OLM, Glyceryl Mono Stearate, Poloxamer 188 and ternary physical mixture of the three mixed powders in ratio of (1:1:1).

Preparation of lipid nanoparticles

The homogenization followed by ultrasonication method was adapted in the present study because it is simple and reproducible method of preparation of both NLC and SLN. The drug (OLM) and the solid lipid (GMS) form the lipid phase of the SLN and (Oleic acid or Capryol 90) were as liquid lipid in NLC). The surfactant (Poloxamer 188 or Tween 80) and water constitute the aqueous phase. Accurately weighed components of the oily phase were added into small glass bottles. The mixture in the bottle was heated to 80° C, a temperature which exceeds the melting point of the lipid (GMS) which is 69.1° C.

The aqueous phase was prepared by dissolving surfactant in distilled water (20 ml) and heated to the same temperature of oil phase. The aqueous phase was then added to the oily phase and homogenized using Heidolph silent crusher® homogenizer at 20,000 rpm for 10 mins. The obtained coarse emulsion is then sonicated using Branson sonifier®450. The sonication time was 15 minutes, on which the sonication power was set at 90% of maximum output. After sonication, nanoparticles were formed by congealing the sonicated dispersions for 2 hours at 4° C. The preparations were stored in tightly sealed amber glass bottles at refrigerator temperature [8-10].

There are many factors that affect the formulation, the size and in vitro behavior of lipid nanoparticles, among these factors: concentration of the drug, types of lipids, presence of liquid lipids and type and concentration of surfactant, etc. [11-13]. In this study, the three independent variables were studied:

a) Type of surfactant: two non-ionic surfactants were used: Poloxamer 188 or Tween 80.

b) Concentration of surfactant: the high level of this variable was the use of surfactant in concentration of 0.5%, while the low level is 0.25%.

c) Concentration of drug incorporated: two concentrations of OLM were used: low concentration of 0.05% w/v or high concentration of 0.1% w/v of OLM. Due to the change in the drug concentration, two different ratios of drug to lipid were used; these

values are 1:10 and 1:5 respectively. The resultant 8 SLN and 8 NLC formulae are listed in table 1 and 2. Due to presence of liquid lipid in NLC, this variable was replaced by the type of liquid lipid used (Capryol 90 or Oleic acid) as an attempt for improving its gastrointestinal uptake and oral bioavailability and also to control its release.

Characterization of OLM Lipid Nanoparticles

1) Particle Size Analysis

This analysis is used to determine the mean diameter of the nanoparticles and the polydispersity index (PI) which is a measure of the width of the size distribution.

Particle size analysis of SLN and NLC was performed by laser diffraction (LD) using NICOMP 380 ZLS, Dynamic light scattering (DLS) instrument (PSS, Santa Barbara, CA, USA), using the 632 nm line of a HeNe laser as the incident light with angel 90o and Zeta potential with external angel 18.9°. Samples were prepared by 0.2g / 5ml Millipore water and sonication for 5minutes.

2) Zeta Potential

Zeta potential was measured by determining the electrophoretic mobility using NICOMP 380 ZLS, Dynamic light scattering (DLS) instrument (PSS, Santa Barbara, CA, USA), using the 632 nm line of aHeNe laser as the incident light with angel 90o and Zeta potential with external angel 18.9°. Samples were prepared by 0.2g / 5ml Millipore water and sonication for 5minutes. High zeta potential indicates highly charged particles. Generally, high zeta potential (negative or positive) prevents aggregation of the particles due to electric repulsion and electrically stabilizes the nanoparticles dispersion [14]

3) Transmission electron microscopy examination of nanoparticles

Drug loaded nanoparticles are scanned morphologically by Transmission Electron Microscopy (TEM). The transmission microscope used was model JTEM-1010, JEOL®. The operation is done using a negative staining method [15]. A drop of the nanoparticles dispersion was put on copper grid coating, and then the excess droplets were removed using filter paper. After 5 min, a drop of uranyl acetate solution (2% w/v) was then dropped onto the grids. After the samples being negatively stained and air-dried at room temperature, they were ready for the TEM investigation at 74 kV.

4) Entrapment efficiency of OLM in Lipid nanoparticles(LN)

The entrapment efficiency (EE) was determined as described in Yang et al., with some modifications [16]. The desired amounts of LN were dispersed in phosphate buffer solution (pH 6.8). Then they were

vortexed for 5 min to dissolve the free OLM. The dispersion was centrifuged at 15,000 rpm for 30 min. This cause separation of the free OLM from OLM loaded in LN. After separation and suitable dilution,

the amount of the free OLM in the dispersion medium was estimated by UV spectrophotometer. OLM entrapment efficiency was calculated from the following equation:

$$\text{Entrapment Efficiency (\%)} = \frac{W_{\text{total (OLM)}} - W_{\text{free(OLM)}}}{W_{\text{total (OLM)}}} \times 100$$

$W_{\text{total(OLM)}}$ and $W_{\text{free(OLM)}}$ are the weight of drug added in system and analyzed weight of drug in supernatant respectively.

5) In Vitro Release of OLM from the prepared Lipid nanoparticles

The in vitro release of OLM was evaluated by the dialysis method as reported by **yang et al.**, and **Das et al.**, with slight modifications ^[16 and 17].

The dialysis membrane was soaked in the release medium (phosphate buffer, pH 6.8) for 24 hours before the experiment. Accurately measured one milliliter of the formulations and marketed product was placed in the dialysis tube. The membrane was thoroughly tied to prevent leakage of the drug. The dialysis tube was put in a beaker containing 50 ml of the release medium. The beaker was protected from light and kept horizontally on a Clifton® shaking water bath rotating at 100 rpm for 12 hours. At predetermined time intervals (0.5, 1, 2, 4, 6, 8 and 12 hours). Five ml release medium samples were withdrawn and replaced by the same volume of fresh release medium. The samples were diluted to a suitable concentration, then analyzed using UV spectrophotometer as described before. The experiments were done in triplicates and the mean ± SD was calculated using Microsoft office excel, 2013.

RESULTS AND DISCUSSION

Preformulation study of OLM

Fourier Transform Infrared spectroscopy of OLM

The FTIR Spectroscopy is done on pure OLM powder, GMS and Poloxamer 188, and the physical mixture of the drug and the two solid ingredients to investigate possible incompatibilities between the drug and those additives before formulation

Fig. 1 shows the FTIR spectrum of OLM. The IR spectrum of OLM revealed a characteristic peak at 3419 cm^{-1} for O-H group, a peak at 3290 cm^{-1} for N-H group and two characteristic sharp peaks at 1831 cm^{-1} and 1706 cm^{-1} for two C=O groups. The spectrum of OLM also showed aromatic C=C stretching at (1550 cm^{-1} , 1532 cm^{-1} , 1474 cm^{-1}) and $\text{sp}^2\text{C-H}$ stretching at (3040 cm^{-1} , 3000 cm^{-1}). In addition, the spectrum showed six peaks for C-O stretching at (1299 cm^{-1} , 1227 cm^{-1} , 1170 cm^{-1} , 1135 cm^{-1} , 1087 cm^{-1} , 1052 cm^{-1}) as presented in fig. 1.

For the solid lipid GMS, As shown in fig. 2, the O – H stretching vibration of GMS appeared at 3306 cm^{-1} as a broad peak and C-H stretching at 2408 cm^{-1} , while the peak corresponding to C = O group appeared at 1730 cm^{-1} . The FTIR spectrum of GMS was found to be identical with the spectra in number of pharmaceutical books such as handbook of pharmaceutical excipients ^[19] and analytical books as UV and FTIR spectra of pharmaceutical substances. Poloxamer 188 is considered as a grade of the pharmaceutical excipients category Poloxamer. The Poloxamer polyols are a series of closely related block copolymers of ethylene oxide and propylene oxide conforming to the general formula: HO – (C₂H₄O)_x (C₃H₆O)_y (C₂H₄O)_z – H.

As shown in fig. 3, The FTIR spectrum of Poloxamer 188 shows three characteristic IR bands. The band corresponding to O – H group is appeared as a broad band at 3448 cm^{-1} . The band specific for the C – H stretching is an intense band of wave number 2887 cm^{-1} . The third important functional group is C – O having intense band at 1111 cm^{-1} . These findings are in complete agreement with the FTIR study of Poloxamer 188 which have been conducted by **Karekar et al.**, (2009) ^[20]

The FTIR spectrum of the binary physical mixture of OLM and GMS is shown in fig. 4. Combination of peaks characteristic for the functional groups in both substances observed. All characteristic peak of pure OLM observed as it is. A characteristic peak at 3419 cm^{-1} for O-H group, a peak at 3290 cm^{-1} for N-H group and two characteristic sharp peaks at 1831 cm^{-1} and 1706 cm^{-1} for two C=O groups. The spectrum of OLM also showed aromatic C=C stretching at (1550 cm^{-1} , 1532 cm^{-1} , 1474 cm^{-1}) and $\text{sp}^2\text{C-H}$ stretching at (3040 cm^{-1} , 3000 cm^{-1}). In addition, the spectrum showed six peaks for C-O stretching at (1299 cm^{-1} , 1227 cm^{-1} , 1170 cm^{-1} , 1135 cm^{-1} , 1087 cm^{-1} , 1052 cm^{-1}).

All peaks of both substances appeared in their same wave length – although there is small change in peak intensity – indicating complete compatibility between the two substances.

The binary physical mixture between OLM and Poloxamer 188 showed similar behavior as the OLM - GMS mixture. It showed the appearance of the same bands of each single component with slight

change in intensity of certain peaks; this reduced intensity is related to dilution of the components of the mixture. As shown in fig.5, a diffused peak showing the O – H stretching of both substances into a broad peak at the same wave number 3477 cm⁻¹. Vibration peak C- H stretching appeared in pure Poloxamer 188 spectrum in (fig. 3) was appeared in the spectrum of the mixture in the same wave number 2887 cm⁻¹. All other peaks of both substances appeared unchanged.

Fig. 6 shows the FTIR spectrum of the ternary physical mixture of the three powders. It shows a combination of all bands that was present in the spectra of each single powder with slight change in intensity. In the figure, the O - H stretching of the three powders and N - H stretching of OLM are appeared in the same range. C - H stretching vibration in Poloxamer 188 and C - H stretching vibration in GMS appeared in the same range. It could be concluded that the use of these solid substances concomitantly is of no compatibility problems.

Preliminary differential scanning calorimetry study

The DSC thermogram of OLM, GMS, and Poloxamer 188 and the ternary physical mixture composed of the three substances in a ratio of (1:1:1) are collectively shown in figures (7-10).

From the separate DSC thermogram of the pure substances shown in figures (7-10), DSC thermograms of pure OLM, GMS and Poloxamer 188 show endothermic peaks at 179, 69.1 and 54.92 °C, respectively, corresponding to their melting points. Japanese pharmacopeia and USP -31 have stated that the melting point of Glyceryl Mono Stearate is not below 55 °C [21 and 22]. More specific results are obtained by **Yahjma et al., (2002)** [23] who have mentioned two values of endothermic peaks corresponding to two different forms of GMS. They mentioned that the endothermic peak of α form of GMS was at 67.9 °C, while the endothermic peak of the β form appeared at 71.9 °C. Another close value was mentioned by **Hussain et al., (2003)** [24] who have stated that the endothermic peak of GMS was at 65.4 °C. BASF® technical information leaflet issued February 2010 mention that the melting point of Poloxamer 188® is 52 °C, while the hand book of pharmaceutical excipients specifies a range of 52 – 57 °C as a range for the melting peak of Poloxamer 188^[18].

In the physical mixture of the three substances the endothermic peaks of pure OLM, GMS and Poloxamer were at 189, 158 and 61 °C respectively,. The peak appeared at 61 °C is almost identical to the pure Poloxamer 188 endothermic peak.

The peak of GMS describes a shift of GMS peak to a higher temperature of 158° C, while OLM had a smaller shift but to a higher temperature of 189 °C. The presence of peaks of the three crystalline substances indicates that there is no true complex formed and the drug remains in crystalline form.

Preparation of OLM loaded SLNs and NLCs

OLM loaded SLNs and NLCs were successfully developed using high shear homogenization coupled with ultrasound method. An o/w nanoemulsion was obtained as a clear solution after addition of heated aqueous phase to oily phase, maintained at temperature of 80°C. The SLNs and NLCs were obtained immediately by cooling hot nanoemulsion all prepared formulae were photographed and their photos are shown in fig. 11 .The composition of each formula in each system illustrated in Tables 1 and 2.

Characterization of OLM Lipid Nanoparticles

Particle size, particle size distribution and Zeta potential (ZP) of the prepared OLM-LNs

Particle size was determined and the average diameter was measured in nanometers, while particle size distribution was evaluated by the polydispersibility index. Particle size, polydispersibility index and zeta potential data are listed in Table 3.

The particle size of SLN formulations ranged from 219.9 nm to 363.5 nm for SLN-2 and SLN-3 respectively, while the particle size of NLC formulations ranged from 176.8 nm to 382.2 nm for NLC-2 and NLC-7 respectively. Particle size distribution is one of the most important characteristics for the evaluation of the stability of the colloidal systems. The PDI gives information about the homogeneity of particle size distribution in the system. A small value of PDI is an indication of narrow size distribution in the system whereas large value indicates wide size distribution in the system. The particle size distribution of SLNs formulae was narrower than that of NLCs formulae.

The results showed that increasing surfactant concentration, the particle size of nanoparticles decreased. It may be attributed to effective reduction in interfacial tension between the aqueous and lipid phases leading to the formation of emulsion droplets of smaller size. . Using Tween 80 as surfactant resulted in smaller particle size, as Tween 80 showed lower HLB and more lipophilicity than Poloxamer 188. Tween 80 has HLB value of 15, while according to the manufacturing company of Poloxamer 188 its HLB is > 24^[25]. It is obvious that there is no distinct effect of the amount of the drug incorporated on the particle size. The higher viscosity of oleic acid at 20°C (36.56 cps) when compared

Capryol 90 (30 cps) at the same temperature [26]. Consequently, this could be considered as the most important factor for the larger size of oleic acid-NLCs. Hence, the mean particle size of lipid nanoparticles usually increased with increasing viscosity of the oil phase.

Transmission electron microscopy examination of SLN nanoparticles

The TEM photographs of the prepared formulae are shown in fig. 12. Photos taken by TEM were magnified 80000 times. From these figures, The TEM investigation revealed that the OLM-SLN nanoparticles were homogenous and spherical or ellipsoidal in shape except formulae SLN-5, SLN-6, SLN-7, and SLN-8 were slightly of non-spherical (anisometric) shape. This finding suggests that higher amount of drug included in these SLN formulae may have an effect on the polydispersibility of the lipid by affecting the polymorphic nature of it. The TEM investigation also revealed that the OLM-NLC nanoparticles were homogenous and spherical or ellipsoidal in shape. This indicates good homogeneity and good uniformity that may result in uniform release of the entrapped OLM.

Entrapment efficiency of OLM –SLNs and OLM-NLCs

The measured entrapment efficiencies of OLM in the prepared LNs are listed in Table 4. The EE% for various factor level combinations was found for SLNs and NLCs in the range of 63.23 % to 84.55 % and 77.05 to 90.64 respectively. The values of entrapment efficiency of OLM-NLCs were higher than in OLM-SLNs. It could be attributed to the presence of the liquid nano compartments formed by Capryol 90 or oleic acid, which were entrapped within the solid matrix of the NLCs. So, NLCs served as nanoreservoir drug delivery systems for OLM.

The results showed that increasing surfactant concentration, the entrapment efficiency of nanoparticles decreased. This observed decrease in E.E. % could be explained by partition phenomenon. High surfactant level in the external phase might increase the partition of drug from internal to external phase of the medium. This increased partition is due to the increased solubilization of the drug in the external aqueous phase so more drug can disperse and dissolve in it [27]. Formulations containing Tween 80 as surfactants showed higher entrapment efficiency compared to the other surfactants; this could be due to the lower HLB value

of Tween 80. Percentage of OLM to be entrapped was found to be higher in SLNs formulae containing lower amount of drug, this may be due to limited number and space inside SLNs nanoparticles which liable to be occupied by the drug.

In Vitro Release of OLM from the prepared LNs

In vitro release study using dialysis bag diffusion technique has been performed over 12 hrs, each sample was analyzed in triplicate and the release curves are shown in Fig (13 and 14). The OLM release from SLNs was quite faster than its release from NLCs; which could be due to the higher entrapment efficiency and drug loading of NLCs due to presence of liquid lipids.

Incorporation of Capryol 90 or oleic acid which are spatially incompatible liquid lipids, which lead to high loading capacity and decreased leakage of the drug from the matrix. So, in SLNs higher amount of drugs leaked from the lipid matrix which will be released in higher rate than that present throughout the lipid matrix.

As shown in Fig (13 and 14), OLM lipid nanoparticles formulations were able to release OLM in controlled manner and the percentage of OLM released up to 12 hours ranged from 77.64 to 98.69% and from 57.8 to 72.2% for SLN and NLC formulations respectively. Interestingly, the amount of poloxamer 188 used had a great influence on the release pattern LNs. Increasing the surfactant concentration led to corresponding increase in the percentage of OLM released. The fast or rapid release and higher release efficiency noticed at higher surfactant concentration could be explained by the partitioning effects of the drug between the melted lipid phase and the aqueous surfactant phase during particle production. During particle production by the hot homogenization technique, drug partitions from the liquid oil phase to the aqueous water phase. The amount of drug partitioning to the water phase will increase with the increase of the drug solubility in the water phase, which means with increasing temperature of the aqueous phase and increasing surfactant concentration. The higher surfactant concentration, the greater is the solubility of the drug in the water phase so the amount of drug in the outer shell increased and released in a relatively rapid way [28].

Table 1: Composition of prepared OLM-SLN formulae

	OLM (W/V%)	GMS (mg)	Tween 80 (mg)	Poloxamer188 (mg)
SLN-1	0.05	100	50	
SLN -2	0.05	100	100	
SLN -3	0.05	100		50
SLN -4	0.05	100		100
SLN -5	0.1	100	50	
SLN -6	0.1	100	100	
SLN -7	0.1	100		50
SLN -8	0.1	100		100

Table 2: Composition of prepared OLM-NLC formulae

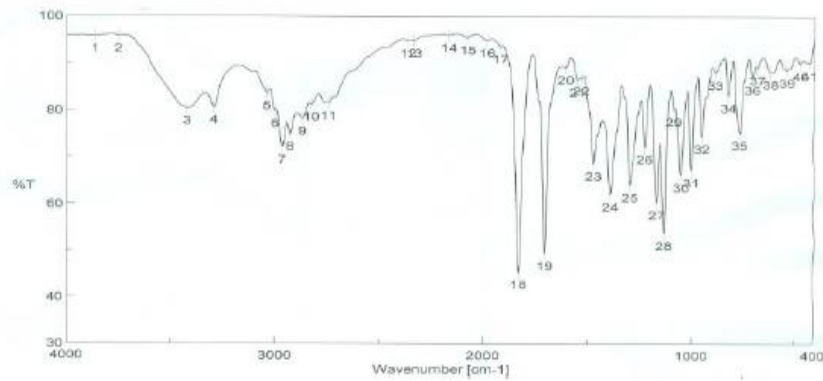
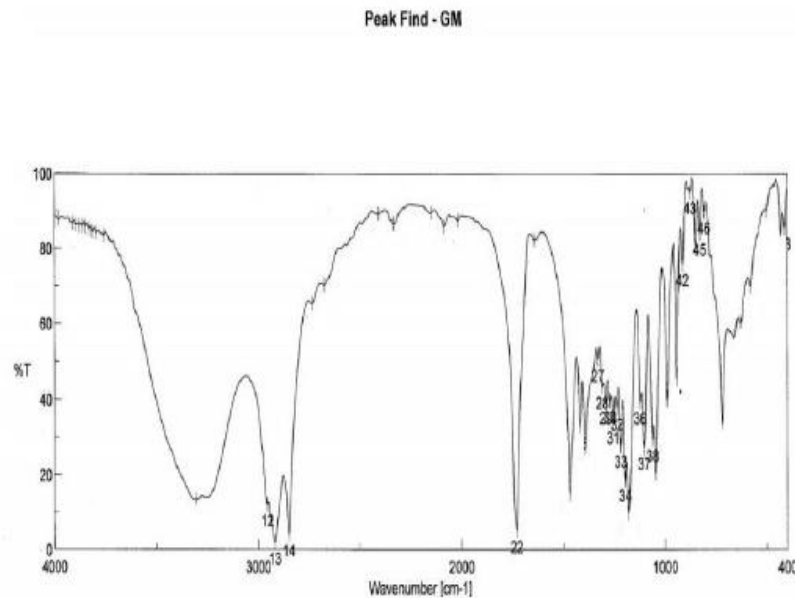
	OLM (mg)	GMS (mg)	Capryol 90 (mg)	Oleic acid (mg)	Tween 80 (mg)	Poloxamer188 (mg)
NLC-1	10	70	30		50	
NLC-2	10	70	30		100	
NLC-3	10	70	30			50
NLC-4	10	70	30			100
NLC-5	10	70		30	50	
NLC-6	10	70		30	100	
NLC-7	10	70		30		50
NLC-8	10	70		30		100

Table 3: Particle size, Polydispersibility index and zeta potential values of the prepared LNs

Batch NO.	SLN Formulae			NLC Formulae		
	Particle size(nm)	PDI	ZP	Particle size(nm)	PDI	ZP
F1	285.8	0.46	-20.6	223.6	0.657	-18.4
F2	217.9	0.271	-18.7	176.8	0.672	-21.9
F3	334.5	0.351	-21.1	252.1	0.63	-24.7
F4	261.2	0.426	-22	214.2	0.473	-20.8
F5	309.8	0.434	-24	321.1	0.565	-24.7
F6	221.5	0.192	-16.7	280	0.353	-25.8
F7	328.4	0.387	-22.6	382.2	0.271	-27.9
F8	224.4	0.316	-19.4	292.5	0.45	-21.8

Table 4: Entrapment efficiency of the prepared LNs

Batch NO.	SLN Formulae	NLC Formulae
	Entrapment efficiency (%)	Entrapment efficiency (%)
F1	84.55	90.64
F2	70.58	88.5
F3	80.88	89.76
F4	67.35	87.82
F5	75	84.11
F6	66.17	82.88
F7	72.05	83.41
F8	63.235	77.05


Fig. 1: FTIR spectrum of Pure OLM

Fig. 2: FTIR spectrum of GMS

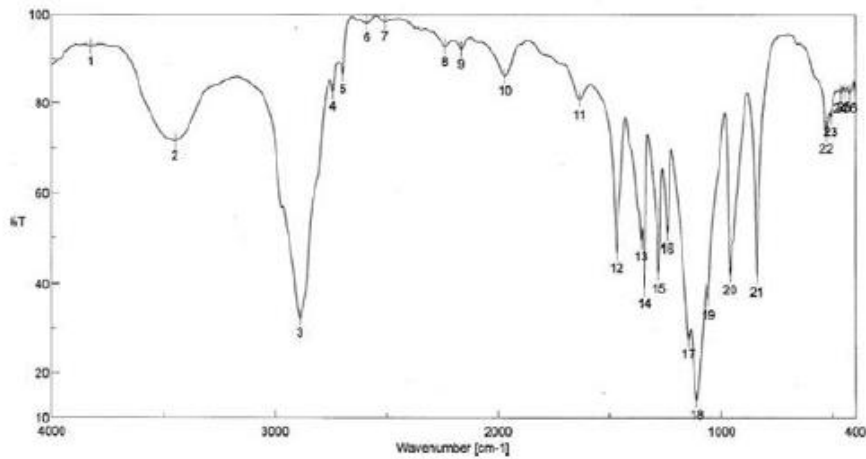


Fig.3: FTIR spectrum of Poloxamer 188

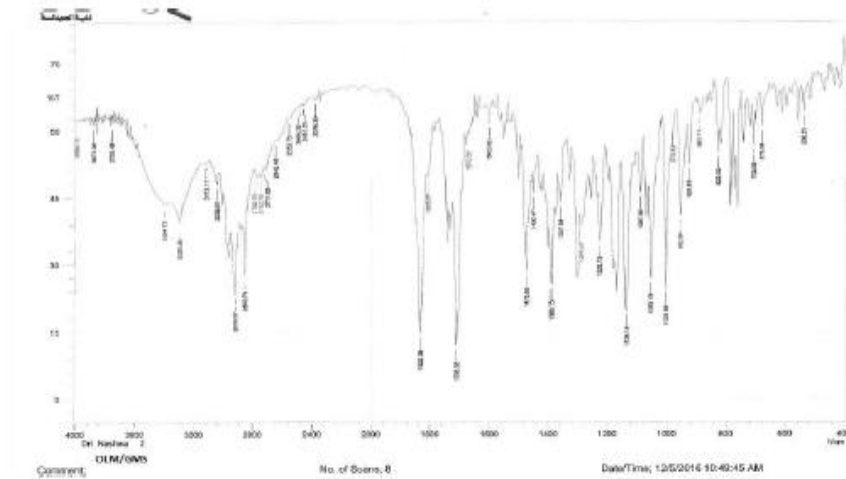


Fig. 4: FTIR spectrum of binary mixture of OLM and GMS

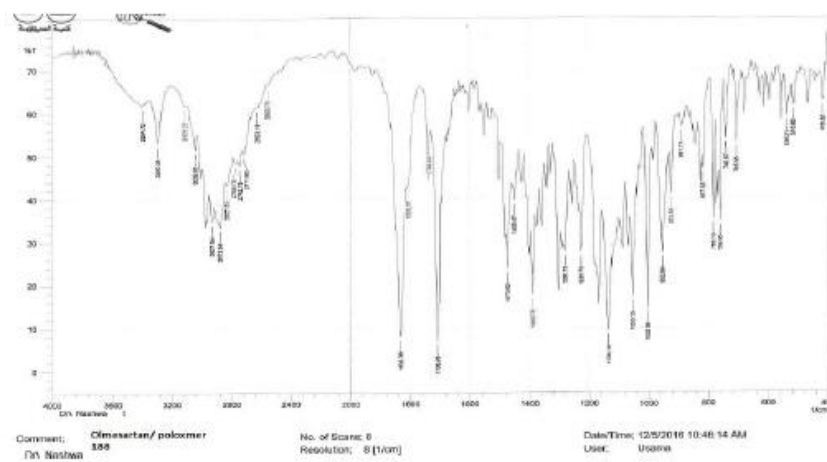


Fig. 5: FTIR spectrum of the binary mixture of OLM and Poloxamer 188

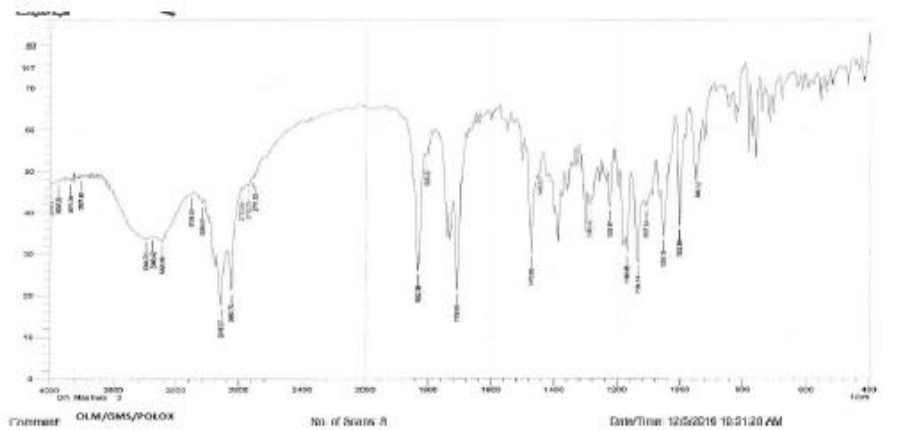


Fig. 6: FTIR spectrum of the ternary physical mixture containing OLM, GMS and Poloxamer 188

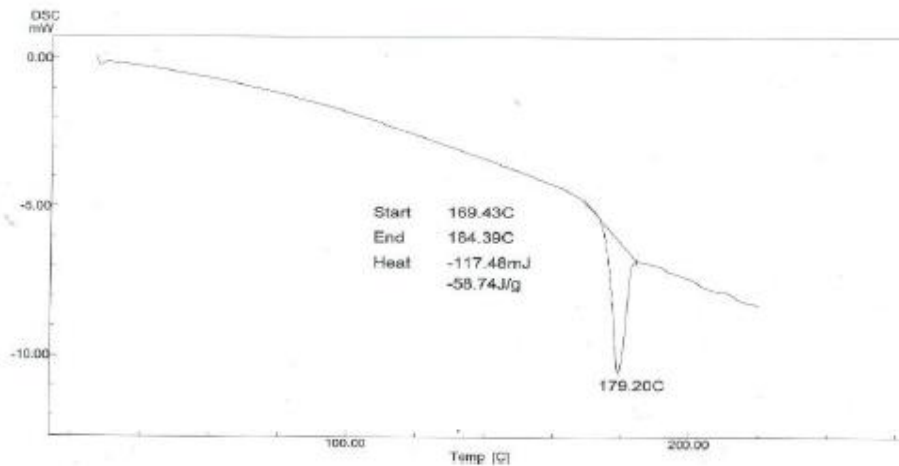


Fig. 7: DSC thermograms of pure OLM

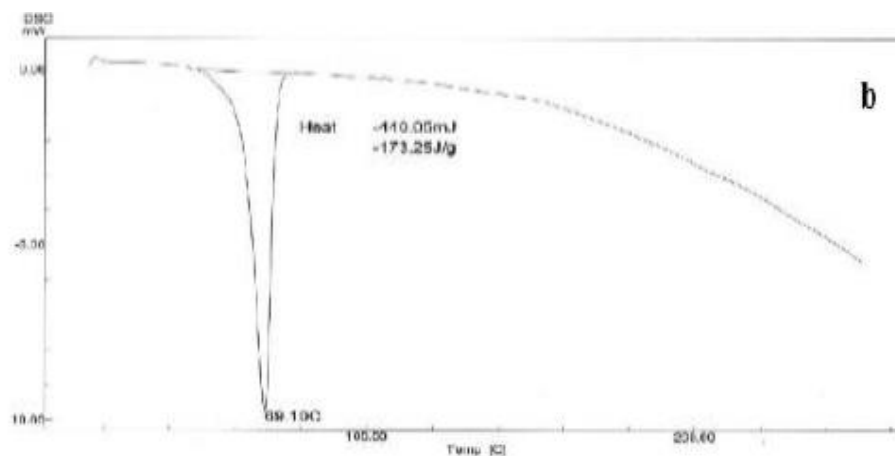


Fig. 8: DSC thermograms of pure GMS

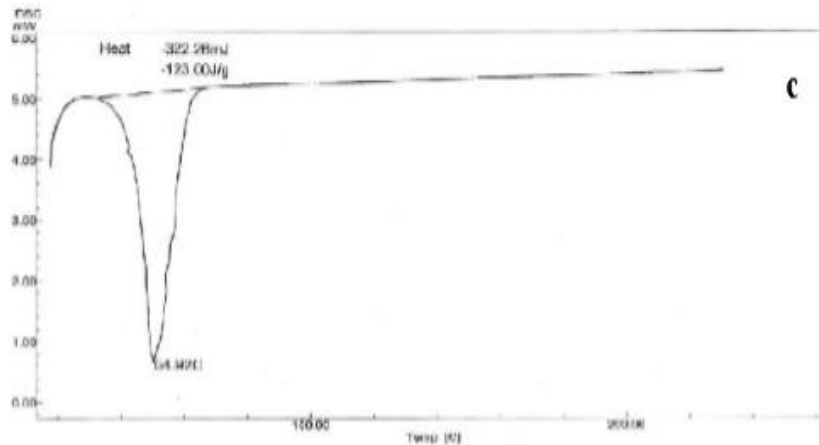


Fig. 9: DSC thermograms of pure Poloxamer 188 separately

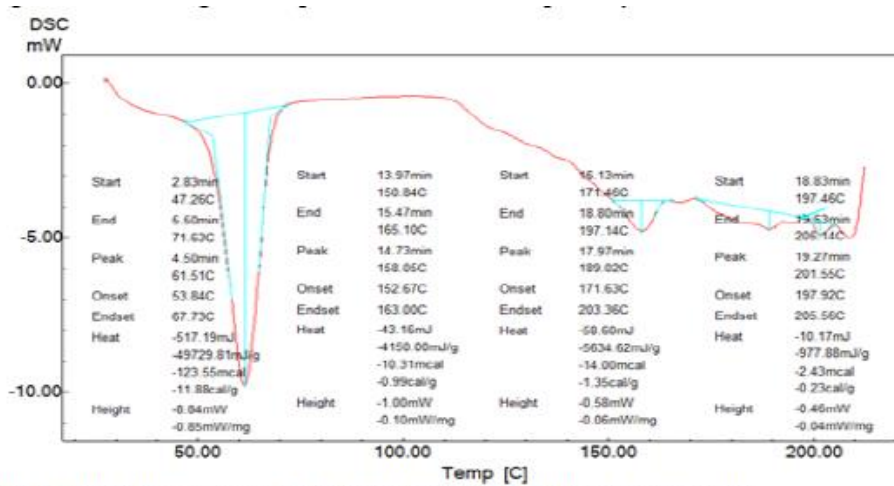


Fig. 10: DSC thermograms of ternary mixture of the three components

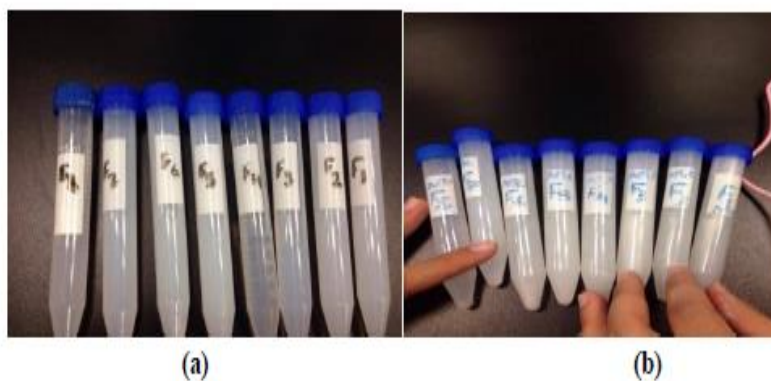
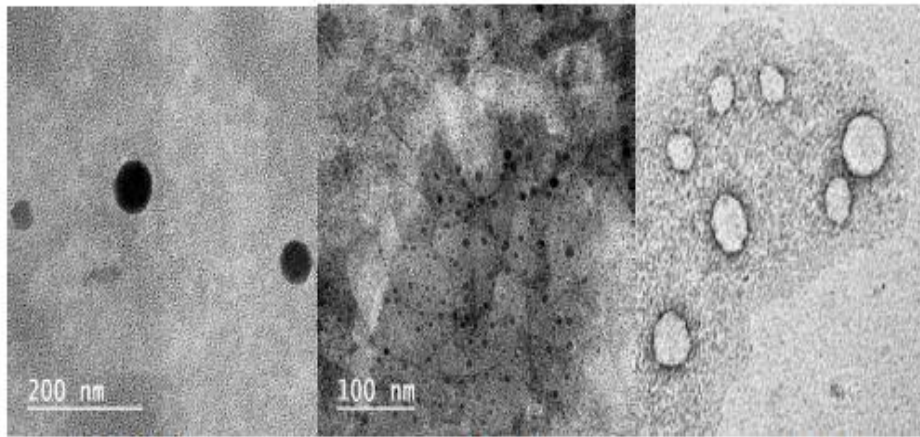


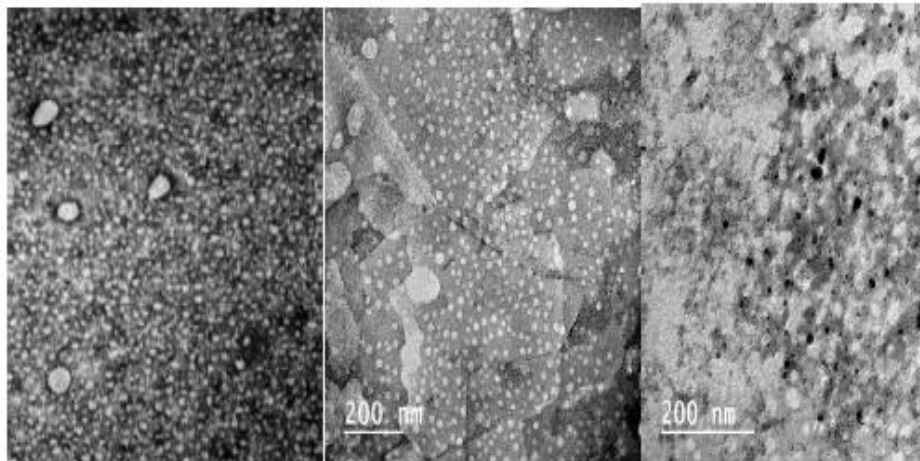
Fig. 11: (a) A photograph of SLNs formulae, (b) A photograph of NLCs formulae



SLN-1

SLN-2

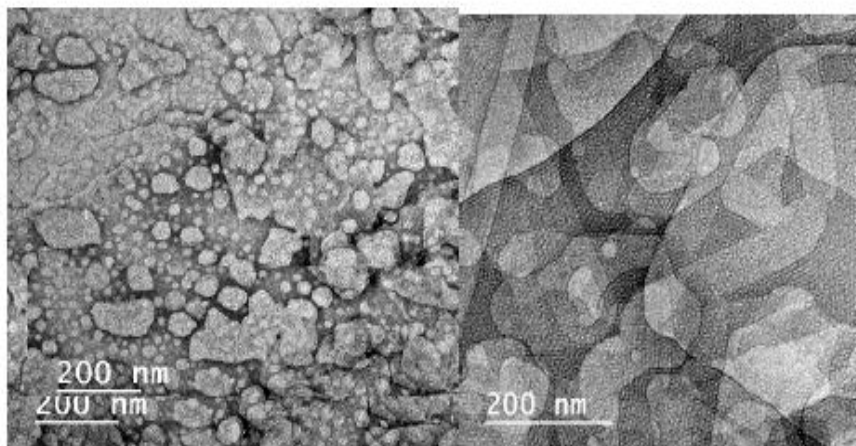
SLN-3



SLN-4

SLN-5

SLN-6



SLN-7

SLN-8

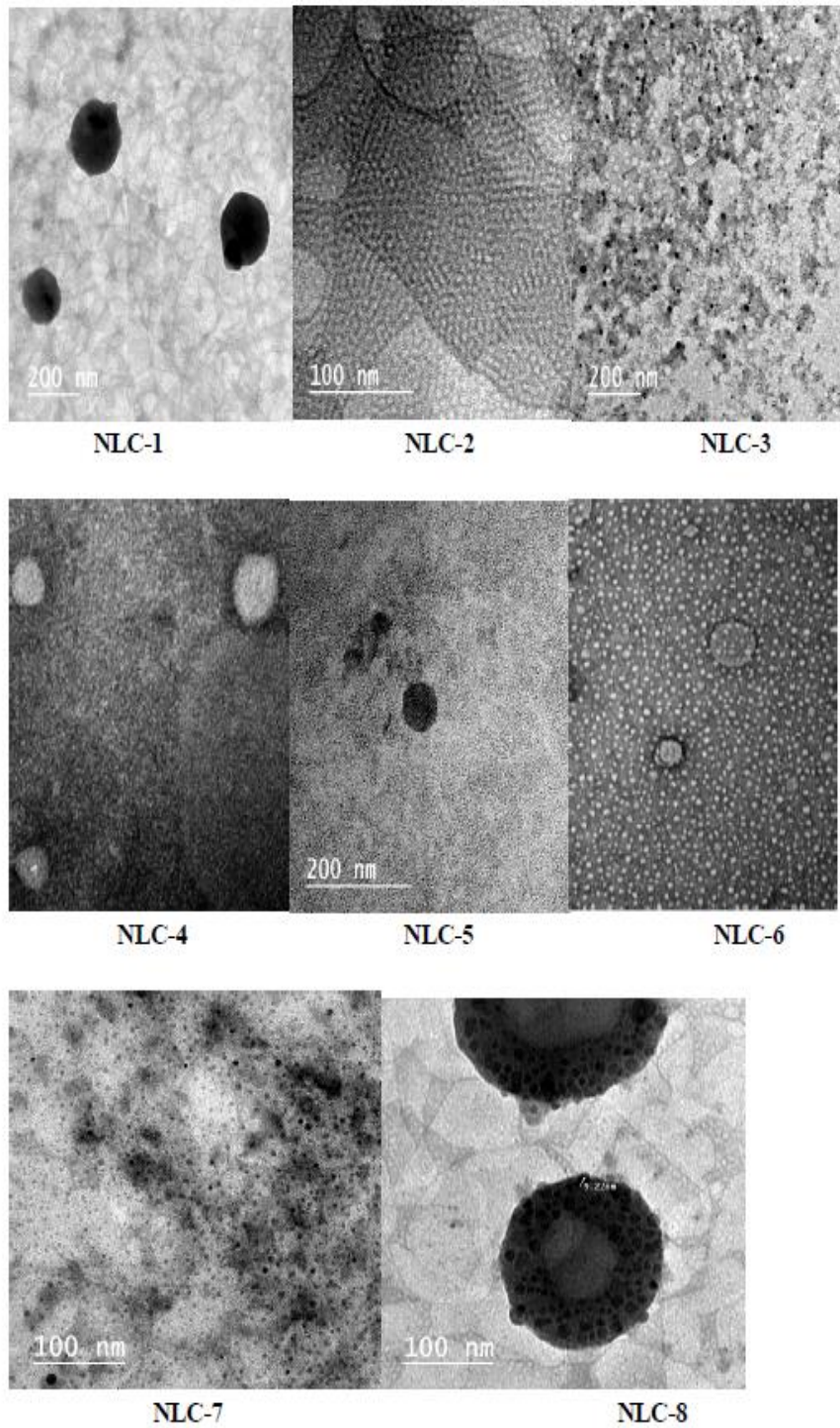


Fig. 12: TEM micrograph depicting the shape and morphology of SLNs and NLCs formulae

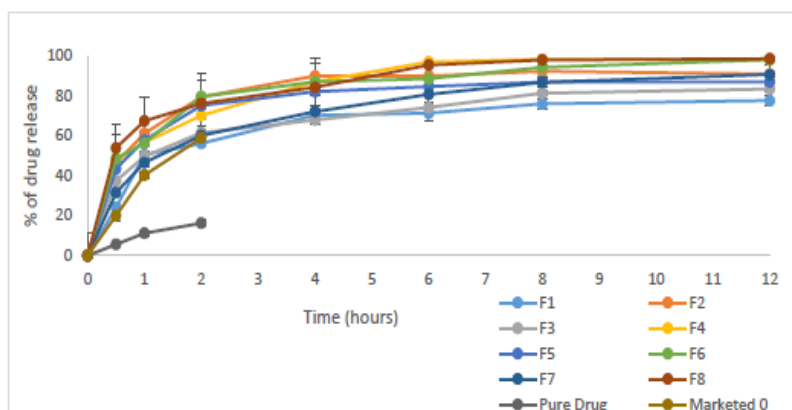


Fig. 13: In vitro release profile of OLM from SLN formulae and compared to pure drug and marketed product

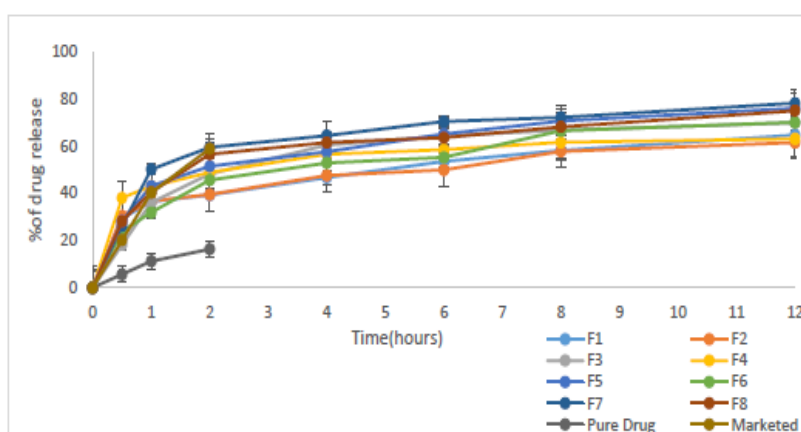


Fig. 14: In vitro release profile of OLM from NLC formulae and compared to pure drug and marketed product

CONCLUSION

In this work, OLM-loaded SLNs and NLCs were successfully prepared by high shear homogenization and ultrasonication technique. The various physicochemical properties, and the in vitro release behavior, were greatly affected and can be controlled by optimizing the compositional variables represented in the type concentration of surfactant and lipid as well as the type of liquid lipid used. The controlled release behavior of OLM loaded LNs with favorable physicochemical characteristics can form a foundation for further clinical studies using these nanoparticles for different fields.

ACKNOWLEDGMENTS

I would like to acknowledge all the members of pharmaceuticals and industrial pharmacy department of the faculty of Pharmacy, Al-Azhar University and

Sinai University for their help and guidance throughout this work. I am grateful to everyone who co-operates in this work.

REFERENCES

- [1]. GT Warne; B Jarvis. *Drugs*, 62, 1345–1353, (2002).
- [2]. CE Baker. *Physician desk reference*, New Jersey, Thomson PDR, (2005).
- [3]. Mukherjee S, Ray S, Thakur R. Solid lipid nanoparticles: A modern formulation approach, in drug delivery system. *Indian J Pharm Sci*; 71: 349-58, (2009).
- [4]. Muller RH, Mader K, Lippacher A, Jenning V. Solid-liquid (semi-solid) liquid particles and method of producing highly concentrated lipid particle dispersions, inPCT/EP00/04565, (2000).
- [5]. Muller RH, Mader K, Lippacher A, Jenning V. Fest-flussige (halbfeste) Lipidpartikel undVerfahren zur Herstellung hochkonzentrierter Lipid partikel dispersion en, inPCT/EP00/04112, (2000).

- [6]. Tang J. (2007), Self-Emulsifying Drug Delivery Systems: strategy for improving oral delivery of poorly soluble drugs, *Current drug therapy*, 2: 85–93.
- [7]. Martins, S. Costa-Lima, S., Carneiro, T., Cordeiro-da-Silva, A., Souto, E.B. and Ferreira, D.C., (2012), Solid lipid nanoparticles as intracellular drug transporters: an investigation of the uptake mechanism and pathway, *International Journal of Pharmaceutics*, 430 (1-2): p. 216-27.
- [8]. M. Burra, R. Jukanti, K.Y. Janga, S. Sunkavalli, A. Velpula, S. Ampati, et al., Enhanced intestinal absorption and bioavailability of raloxifene hydrochloride vialyophilized solid lipid nanoparticles. *Advanced Powder Technology*, (2012).
- [9]. G. Abdelbary and R.H. Fahmy, *Diazepam-loaded solid lipid nanoparticles: design and characterization*. *AAPS PharmSciTech*, (2009). 10 (1): p. 211-9.
- [10]. K. Manjunath and V. Venkateswarlu, Pharmacokinetics, tissue distribution and bioavailability of clozapine solid lipid nanoparticles after intravenous and intraduodenal administration. *Journal of Controlled Release*. 107 (2): p. 215-28, (2005).
- [11]. R. Tiwari and K. Pathak, Nanostructured lipid carrier versus solid lipid nanoparticles of simvastatin: comparative analysis of characteristics, pharmacokinetics and tissue uptake. *International Journal of Pharmaceutics*. 415 (1-2): p. 232-43. *References* 186, (2011).
- [12]. X. Lin, X. Li, L. Zheng, L. Yu, Q. Zhang, and W. Liu, Preparation and characterization of monocaprates nanostructured lipid carriers. *Colloids and Surfaces A: Physicochemical and Engineering Aspects*. 311 (1): p. 106-11, (2007).
- [13]. F. Han, S. Li, R. Yin, H. Liu, and L. Xu, Effect of surfactants on the formation and characterization of a new type of colloidal drug delivery system: nanostructured lipid carriers. *Colloids and Surfaces A: Physicochemical and Engineering Aspects*. 315 (1): p. 210-16, (2008).
- [14]. S. Das and A. Chaudhury, Recent advances in lipid nanoparticle formulations with solid matrix for oral drug delivery. *AAPS PharmSciTech*. 12 (1): p. 62-76, (2011).
- [15]. Zhang, X., Liu, J., Qiao, H. Liu, H., Ni, J., Zhang, W. et al. (2010), Formulation optimization of dihydro artemisinin nanostructured lipid carrier using response surface methodology, *Powder Technology*, 197 (1): 120-28.
- [16]. X.Y. Yang, Y.X. Li, M. Li, L. Zhang, L.X. Feng, and N. Zhang, Hyaluronic acid coated nanostructured lipid carriers for targeting paclitaxel to cancer. *Cancer Letters* 334 (2): p. 338-45, (2013).
- [17]. Das and A. Chaudhury, Recent advances in lipid nanoparticle formulations with solid matrix for oral drug delivery. *AAPS Pharm SciTech*. 12 (1): p. 62-76, (2011).
- [18]. Rowe, R.C., Sheskey, P.J., Quinn, M.E., Association, A.P. and Press, P., *Handbook of pharmaceutical excipients*, Vol. 6. (2009): Pharmaceutical press London.
- [19]. Dibbern, H.W., *UV and IR spectra: Pharmaceutical substances (UV and IR) and pharmaceutical and cosmetic excipients (IR)*. ECV, Editio Cantor-Verlag (2002).
- [20]. Karekar, P., Vyas, V., Shah, M., Sancheti, P. and Pore, Y., (2009), physicochemical investigation of the solid dispersion systems of etoricoxib with poloxamer 188, *Pharmaceutical Development and Technology*, 14 (4): 373-79.
- [21]. United States Pharmacopeia, USP 38, NF 33, (2015). NF. p. 2899.
- [22]. Committee J.P.E., *Japanese Pharmacopoeia*, 16th edition, Hirohawa Press: Tokyo. (2011). p. 704.
- [23]. Yahjima, T., Itai, S., Takeuchi, H. and Kawashima, Y., (2002), Determination of optimum processing temperature for transformation of Glycerol monostearate, *Chemical and Pharmaceutical Bulletin*, 50 (11): 1430-33.
- [24]. Hussain, T., Saeed, T., Mumtaz, A.M., Javaid, Z., Abbas, K., Awais, A., et al., (2013), Effect of two hydrophobic polymers on the release of gliclazide from their matrix tablets, *ACTA Poloniae Pharmaceutica- Drug Research*, 70: 749-57.
- [25]. BASF®, *Lutrol L and Lutrol f grades*. p. 1-8, (2010).
- [26]. D.S. Viswanath, T. Ghosh, D.H. Prasad, N.V. Dutt, and K.Y. Rani, *Viscosity of liquids: theory, estimation, experiment, and data* Springer Science & Business Media. (2007).
- [27]. Rahman Z, Zidan AS, Khan MA. Non-destructive methods of characterization of risperidone solid lipid nanoparticles. *Eur J Pharm Biopharm*, 76, 127-137, (2010).
- [28]. Zur Muhlen A, Mehnert W. Drug release and release mechanism of prednisolone loaded solid lipid nanoparticles. *Pharmazie*, 53, 552-555, (1998).